

Progressive Class-Wise Attention (PCA) Approach for Diagnosing Skin Lesions

Asim Naveed, Syed S. Naqvi, Tariq M. Khan, Imran Razzak

Abstract—Skin cancer holds the highest incidence rate among all cancers globally. The importance of early detection cannot be overstated, as late-stage cases can be lethal. Classifying skin lesions, however, presents several challenges due to the many variations they can exhibit, such as differences in colour, shape, and size, significant variation within the same class, and notable similarities between different classes. This paper introduces a novel class-wise attention technique that equally regards each class while unearthing more specific details about skin lesions. This attention mechanism is progressively used to amalgamate discriminative feature details from multiple scales. The introduced technique demonstrated impressive performance, surpassing more than 15 cutting-edge methods including the winners of HAM1000 and ISIC 2019 leaderboards. It achieved an impressive accuracy rate of 97.40

Index Terms—Deep Learning; Convolutional Neural Networks; Attention Mechanism; Skin Cancer

I. INTRODUCTION

The skin makes up a significant amount of a person's body, accounting for almost 16% of total body weight. The three layers of skin are the epidermis, dermis, and subcutaneous tissues, also referred to as the hypodermis. Thermoregulation, metabolism, sensory perception, and protection are among the most significant skin functions. The skin protects the body against external invasions by acting as a barrier. Blood vessels, lymphatic vessels, nerves, and muscles are all found in the skin, enabling sweat to pass through the pores, regulating body temperature, and protecting the body from external elements. Excessive sun exposure, heat and cold, chemicals, medications and other factors can cause skin diseases [1].

Dermatology is challenging due to the complexity of the diagnostic processes required for skin diagnosis. Due to the complexity of the problem, which involves significant variations in skin tone and other skin diseases, it becomes even more challenging to diagnose the precise forms of the disease. There are currently more than 200 known skin diseases, and the number grows day by day. Nearly 80% of the population has some type of skin disease [2].

In the past three decades, skin cancer has become one of the most lethal and fast-spreading malignancies in the world [3]. Skin cells are classified into three types: squamous cells, basal cells, and melanocyte cells. Melanocytic and non-melanocytic skin cancers are two different forms. Doctors frequently misclassify malignant melanoma as benign since it

is challenging to distinguish melanoma tumours from benign ones. To reduce the risk of death, it is crucial to recognise the right form of cancer at an early stage [4]. Melanoma is the most prevalent cancer that develops in the melanocyte cells and rapidly spreads throughout the body [5]. It is more fatal than basal and squamous cell carcinoma. Any part of the human body can be affected by it. It is most typically found in sun-exposed regions like hands, face, neck, lips, and other similar locations. Melanoma skin cancer is treatable if it is found in its early stages; if not, it can spread to other body areas and result in a painful death [6]. Melanoma skin cancer makes up just 5% of the occurrences of skin cancer overall, but it is more deadly, according to the American Cancer Society [7]. Doctors or dermatologists frequently utilize the ABCDE method (A for asymmetry, B for border, C for colour, D for diameter, and E for evolution) for skin lesions diagnosis. Dermatologists employ the ABCDE assessment criteria to identify skin cancer in its early stages [8]. Owing to the quantitative nature of the problem, there is a lot of interest in the creation of semi or completely autonomous computer-aided diagnostic (CAD) systems. These systems may be applied in different settings such as decision support in screening or as an alternative opinion [9].

Medical image segmentation is a critical tool in healthcare, greatly improving diagnostic and therapeutic processes [10]–[14]. Offering a transparent view of internal bodily formations, such as tumours or lesions, it equips doctors with the capability to make accurate and prompt diagnoses [15]–[18]. Beyond visualization, this method is invaluable in quantifying and presenting anatomical structures, or assessing the size of pathologies like tumours or blood vessels [19], [20], an essential aspect in tracking disease evolution or gauging the effectiveness of treatments.

CAD systems employ a mix of machine learning and digital image processing techniques to aid dermatologists in clinical screening. Early CAD systems used pre-processing, segmentation of skin lesions, and hand-crafted feature extraction of the segmented lesions for skin lesions classification. These methods do not perform well in cases where the lesions have a fuzzy border and the presence of artefacts such as hair and bubbles and ruler marks [21]. Convolutional neural networks (CNN) have regularly been employed to categorise skin lesions [22]. Although CNN-based skin lesions classification networks have obtained promising results, they are not currently applicable in clinical settings. The following factors affect the performance of CAD systems for skin lesions diagnosis: First, the skin lesions are very similar in colour, shape and texture (i.e., low inter-class variation). Second, the high intra-class

Asim Naveed and Syed S. Naqvi are with the Department of Electrical and Computer Engineering, COMSATS University Islamabad (CUI), Islamabad 45550, Pakistan

Tariq M. Khan and Imran Razzak are with the School of Computer Science and Engineering, UNSW, Sydney, Australia

variations within the same class. The two challenges are shown in Figure 1.

The skin lesions data distribution among different classes is highly imbalanced. The data distribution for the categorization of skin lesions is shown in Table I. The NV class, which has more skin lesion samples, may receive greater attention from CNN models than classes with fewer samples. Most CNN networks fail to generalize on the under-represented classes. A few methods used different approaches (e.g., guided loss function [23], [24], auxiliary learning [25]) to handle these issues. Due to the aforementioned problems, the categorization of skin lesions remains a difficult procedure even with image-level supervision.

The proposed method tackles the aforementioned issues by extracting features unique to each class. We observe that each skin lesion class may be represented by a number of feature channels, which aids discrimination of features from various classes. We put forward a unique class-wise attention mechanism that determines the importance of features on an image-by-image basis. Multi-scale class-wise feature information is incorporated in a progressive manner. Depth-wise separable convolution is employed in the proposed class-wise attention mechanism to lower the number of trainable parameters.

Following is a summary of the proposed framework’s main contributions:

- A novel class-wise attention mechanism is proposed to address the issues of inter-class similarity, intra-class variation and class imbalance.
- The proposed class-wise attention mechanism is employed progressively to incorporate relevant features from multiple scales.
- On skin lesions classification benchmarks, the proposed technique obtained state-of-the-art performance in comparison to more than 15 methods from literature including leaderboard winners from ISIC 2019 and HAM10000.

The paper’s main body is organised as shown below: Section 2 discusses the related works. The architecture of the proposed method is described in Section 3. Extensive experimental results and performance comparisons with earlier methods are presented in Section 4. Section 5 provides the conclusion.

II. RELATED WORK

The classification of skin lesions and recent studies using attention mechanisms are briefly reviewed in this section.

A. Skin lesions Classification

Machine learning (ML) based image recognition and classification have emerged as hot topics in a variety of academic areas, particularly with deep learning. For instance, CNNs have shown potential in the classification of skin lesions [26], [27]. However, current research using data-driven models has revealed the best performance results across several test sets ever released. These pre-trained models are often used in conjunction with a Transfer Learning (TL) method [28].

In practice, image classification demands the employment of interpretations that extract discriminatory features within

class variability while preserving informative intra-class variations. Deep neural networks trained by successively using linear and non-linear operations to create hierarchical invariant representations. The majority of image classification problems have general, generalized learnable representations that can be applied to a variety of areas, and they are learnt using different datasets. For the majority of images, data augmentations like translation, rotation, and scale are frequently used when several samples of the same object are included in a database. Utilizing these techniques, the practical implementation of automated skin cancer categorization has substantially improved [24], [29]–[33]. Meanwhile, despite the significant research advancements, a number of variables continue to prevent further improvement in diagnostic performance. The categorization of skin lesions is a difficult process since the images of the lesions typically have poor contrast, fuzzy boundaries, and artefacts including hair, veins, ruler lines, low inter-class variations, substantial intra-class variances, and data imbalance problems. The usage of millions of images in one of the most popular image classification datasets, named ImageNet, demonstrates the requirement for large datasets of images to efficiently train CNN models to learn the properties of the data. [34].

The Deep CNN algorithms have produced impressive classification results, gratitude to preliminary training on this extensive dataset for image classification ([30], [31]). Furthermore, data imbalance affects practically all of the publicly available datasets on skin lesions. Because different forms of skin lesions develop at varying rates and are more or less accessible for image capture, samples within different lesion categories exhibit unequal distributions. Additionally, a number of images show low inter-class variances [35], [36]. These restrictions results in poor performance. Improving the Deep CNN architecture from the initial AlexNet [37] to a more modern model with greater model parameter ability [38] allows for better outcomes on huge image classification tasks. However, it is particularly difficult to enhance performance in small-scale image samples by introducing more parameters, the model could go from a domain with low overfitting risk to one with high overfitting risk [39]. Sometimes, Deep CNNs are utilized in studies that are published in the research without taking the new database of images and the additional intra-class or inter-class changes into account. Techniques that lessen the overfitting issue can be used to prevent these issues [28], [30], [31], [35], [40]. These techniques include data augmentations [41], transfer learning-based processes [28], and multi-target weighted loss functions [23].

B. Deep learning’s based attention mechanisms

The objective of the deep learning attention mechanism is to emulate the human visual attention system by selecting information from a large amount of data that is most related to the current task. Natural language processing and computer vision have both made considerable strides because of it [42]–[44]. Numerous attention-based techniques have recently been developed to improve CNN’s ability to represent features in image classification tasks. A unique residual attention module

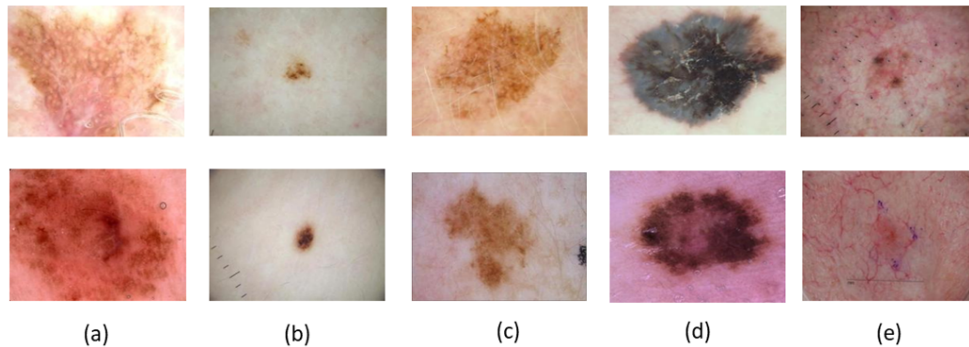


Fig. 1: Low inter-class variations between melanoma (1st row) and non-melanoma (2nd row). High intra-class variations in the same class (a-e).

Class Name	HAM10000		ISIC2019	
	Images	Percentage	Images	Percentage
MEL	1113	11.11%	4522	17.85%
NV	6705	66.95%	12875	50.83%
BCC	514	5.10%	3323	13.12%
AKIEC	327	3.30%	867	3.42%
BKL	1099	11%	2624	10.36%
DF	115	1.20%	239	0.94%
VASC	142	1.40%	253	1%
SCC	-	-	628	2.48%
Total	10015		25331	

TABLE I: Data distribution of HAM10000 and ISIC 2019.

was developed by Wang et al. [45]. The trainable convolutional layers learn the attention weights, and attention feature maps are produced by fusing the convolutional feature maps with the attention weights. A new squeeze and excitation channel-wise attention network (SENet) was proposed by Hu et al. [46]. The attention feature maps in each SE block are created by multiplying the input feature maps by the attention vector that was learnt by two successive fully connected (FC) layers. Numerous attention-based methods for classifying skin lesions have been proposed, another One is ARL-CNN [47]. ARL-CNN can produce attention weights during network training, this reduces the need for processing resources and offers the benefit of avoiding overfitting on small training data sets in contrast to RAN [45] and SENet [46], which learn attention weights via extra learnable layers. Additionally, Through adaptation, ARL-CNN has a large potential to discriminatively concentrate on skin lesion regions. But, one drawback of ARL-CNN is that it only takes into account

spatially focused attention while ignoring crucial channel-wise information. DeMAL-CNN [48] proposed a mixed attention mechanism that takes into account both spatial and channel-wise attention information while building and integrating it into the architecture of each embedding extraction network. This might help DeMAL-CNN better locate skin lesions for CNN. CABNet [49] use global attention and category attention to handle the issue of class imbalance distributions in diabetic retinopathy grading.

III. MATERIALS AND METHODS

In this section, we first go over the benchmark datasets for analyzing skin lesions, then we go over the specifics of the suggested methodology.

A. Skin lesions datasets

The International Skin Imaging Collaboration (ISIC) obtained and assembled the datasets. The HAM10000 [50] was

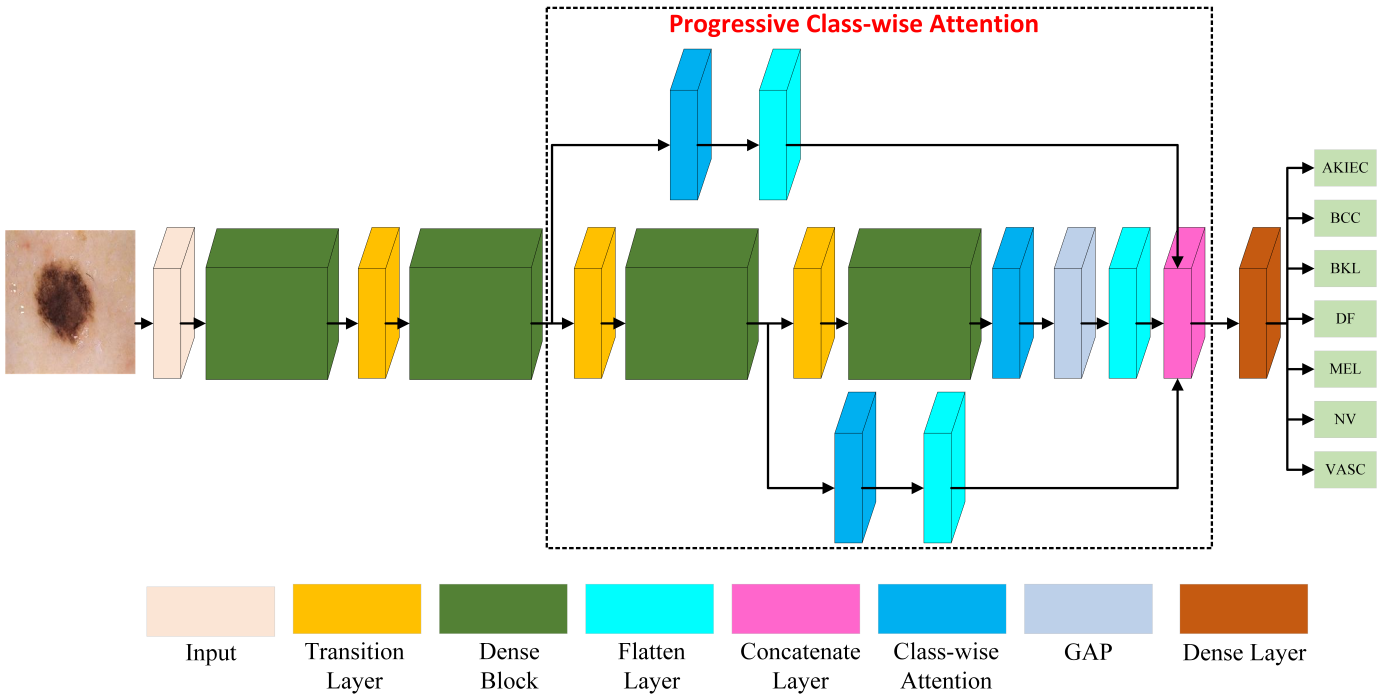


Fig. 2: Block level details of the proposed architecture.

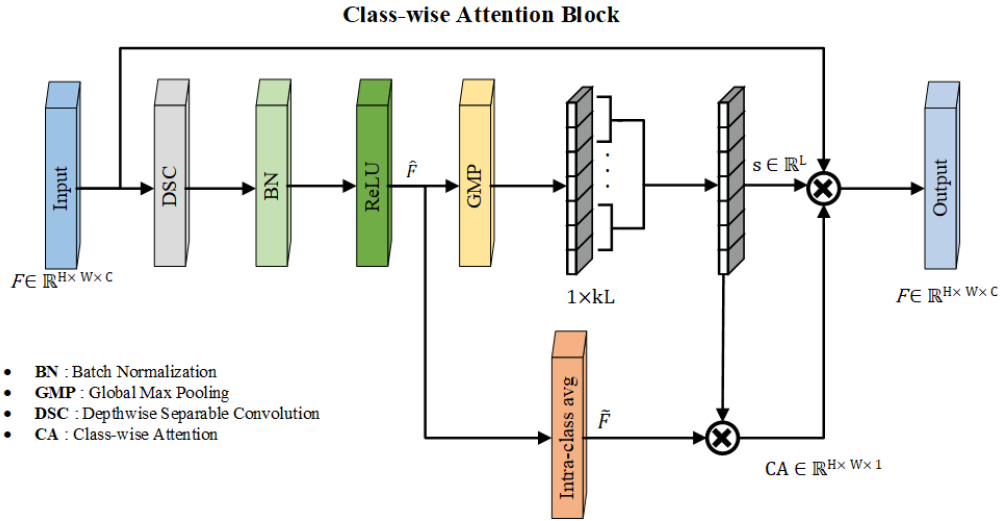


Fig. 3: Details of the proposed class-wise attention block.

presented in 2018 containing 10,015 dermoscopic images and having a size of 450×600 pixels. Seven classes make up the HAM10000: nevus (NV), benign keratosis (BKL), basal cell carcinoma (BCC), dermatofibroma (DF), vascular lesion (VASC), actinic keratosis (AKIEC), melanoma (MEL). The ISIC 2019 [50]–[52] consists of eight classes of dermoscopic images. The classes are nevus (NV), benign keratosis (BKL), basal cell carcinoma (BCC), dermatofibroma (DF), squamous cell carcinoma (SCC), vascular lesion (VASC), actinic keratosis (AKIEC), and melanoma (MEL). The data distribution of each class is present in Table I. The ISIC 2019 and HAM10000 are standard benchmark datasets of dermoscopic images for

comparative analysis of skin lesion analysis methods. From Table I it can be observed the severity of class imbalance in the above-mentioned datasets.

B. Methodology

Traditional CNN-based approaches do not take into account class-related information, therefore their performance is more adversely affected due to the class imbalance problem in skin lesions classification. The proposed technique learns the feature maps in a class-specific approach and treats every type of skin lesion equally.

This is achieved by the proposed class-wise attention technique that associates feature channels with classes equally to reduce channel bias and data redundancy. Results show that class-wise attention mechanisms may effectively address the persistent problems of high inter-class similarity, large intra-class variability, and uneven data distribution in skin lesions classification datasets (Section IV). The details of the proposed network that adopts the DenseNet-121 [53] as its backbone is featured in Figure 2. The details of the class-wise attention mechanism is presented in Figure 3.

1) **Overview of the proposed architecture:** To extract the feature maps from images of skin lesions, the pre-trained DenseNet-121 is employed as the baseline model. The dense connections in the DenseNet architecture allow maximal transmission of skin lesion characteristics across layers through skip connections. Besides, the dense connections can reuse features and diverse features are produced to cater for the multi-scale skin lesion feature extraction for the classification of skin lesions. DenseNet-121 consists of four successive dense blocks and three transition layers. The dense blocks are composed of 12, 24, 48, and 32 densely linked convolutional layers, respectively. To balance the computational load of the dense layers, the three transition layers are responsible for contracting the feature information coming from the dense blocks, by the use of 2×2 pooling layers. We dropped the last three layers of the baseline model and added more layers. The newly added global average pooling (GAP) and classification output layer have replaced the final three layers of the baseline model. The newly added layers reduce the number of parameters of the baseline model while maintaining the performance measures as well.

The proposed class-wise attention is applied progressively to the multi-scale features of DenseNet-121 at multiple stages to getting effective attention feature maps. The choice of the backbone stage that is subjected to attention depends upon the high-level semantic information of the features. The proposed architecture employs class-wise attention after the second, third, and fourth dense blocks, respectively.

Class-wise attention is used to learn various region-wise characteristics for each class. After the class-wise attention mechanism is employed progressively, a global average pooling, and finally a classification layer is used to get the final results.

2) **Class-wise attention mechanism:** To improve the fine-grained classification performance on the specified classes, the class-wise attention mechanism presented in Figure 3 is proposed. It has the ability to distinguish skin lesions on class-based discriminating characteristics.

Let the input tensor from a dense block is represented as $\mathcal{F} \in \mathbb{R}^{H \times W \times C} = \{F_1, F_2, \dots, F_C\}$, where the number of channels, height and width are represented by C, H, and W, respectively. The tensor \mathcal{F} is subjected to a depth-wise separable convolution layer followed by a batch normalization layer and a ReLU activation layer to obtain the tensor $\hat{\mathcal{F}} \in \mathbb{R}^{H \times W \times kL} = \{\hat{F}_1, \hat{F}_2, \dots, \hat{F}_{kL}\}$, mathematically represented as:

$$\hat{\mathcal{F}} = \text{ReLU}(\mu(\mathcal{O}^{3 \times 3}(\mathcal{F}))), \quad (1)$$

where k is the number of feature channels required to find feature maps that can distinguish between each class, L is the number of classes, μ is batch normalization and \mathcal{O} is a depth-wise separable convolution layer. A 3×3 depth-wise separable convolution operation that forms the foundation of our proposed attention technique helps the proposed network to pay attention to specific channels for identifying a particular class. Given the tensor $\hat{\mathcal{F}}$, the score for each class is computed by grouping the channels per class according to k as follows:

$$s_i = \frac{1}{k} \sum_{j=1}^k \delta(\hat{\mathcal{F}}_{i,j}), i \in 1, 2, \dots, L, \quad (2)$$

where δ stands for global max pooling. The class score vector $\mathbf{s} = [s_1, s_2, \dots, s_L]$ signifies the importance of each class for a particular sample.

The class-wise semantic feature map $\tilde{\mathcal{F}} \in \mathbb{R}^{H \times W \times L}$ is computed by averaging the per class maps as follows

$$\tilde{\mathcal{F}} = \frac{1}{k} \sum_{j=1}^k \hat{\mathcal{F}}_{i,j}, i \in 1, 2, \dots, L, \quad (3)$$

The class-level attention map CA is obtained as per equation 4

$$CA = \frac{1}{L} \sum_{i=1}^L \mathbf{s} \tilde{\mathcal{F}}. \quad (4)$$

The discriminative regions that are informative for skin lesions classification are highlighted in CA . Finally, equation 5 applies the class-wise attention to the input tensor \mathcal{F}

$$\mathcal{F}_{CA} = \mathcal{F} \otimes CA, \quad (5)$$

where the final output feature tensor after class-wise attention is \mathcal{F}_{CA} and \otimes stands for element wise multiplication.

3) **Loss functions:** The focal loss [54] is employed for multi-class classification as described in Eq. 6.

$$\mathcal{L}_{\text{focal}} = - \sum_{i=1}^N (1 - \hat{p}_y)^\gamma \log(\hat{p}_y), \quad (6)$$

where \hat{p} is the probability estimate for class y . In our approach, γ serves as a weighting factor for the challenging samples and is empirically determined to be 2.

IV. EXPERIMENTS AND RESULTS

This section reports the outcomes of the proposed approach on benchmark datasets relevant to skin lesions classification, including the ablation study and qualitative and quantitative findings. For interpretability of the learned solution, Grad-CAM [55] is used to obtain the attention maps of the proposed framework.

A. Implementation details

This section outlines the proposed approach implementation details using benchmark datasets for skin lesions classification. Based on prior works [2], [25], [56], we up-sampled the datasets by duplicating the images of minority classes to equal the images in the majority class (i.e., NV class). Afterwards,

Methods	A_{cc}	P_r	S_n	F_1	AUC
baseline (DenseNet-121)	0.889	0.900	0.888	0.887	0.993
baseline+class-wise attention after 4th dense block	0.958	0.963	0.957	0.957	0.997
baseline+class-wise attention at progressive positions	0.973	0.973	0.973	0.972	0.998

TABLE II: Progressive class-wise attention.

Method	Runs	A_{cc}	P_r	S_n	F_1	AUC
PCA	First	0.9768	0.9777	0.9768	0.9763	0.9981
	Second	0.9734	0.9739	0.9734	0.9728	0.9976
	Third	0.9778	0.9781	0.9778	0.9774	0.9982
	Fourth	0.9720	0.9729	0.9719	0.9713	0.9977
	Fifth	0.9713	0.9712	0.9713	0.9709	0.9977
Proposed (ours)		0.9743 ± 0.0029	0.9748 ± 0.0030	0.9742 ± 0.0029	0.9737 ± 0.0030	0.9978 ± 0.0027

TABLE III: Average results of the proposed method on HAM10000 over five training runs along with the standard deviation.

the datasets were divided into three sections: 20% for test, 20% for validation, and 60% for training.

To overcome the issue of less data, we performed data augmentation to enhance data diversity including data rotation from 0 to 180 degrees, width and height shift, zoom in and out, and horizontal and vertical flip. Before augmentation, the datasets were resized to 224×224 pixel resolution. We employed focal loss with Nadam optimizer for the period of 40 iterations with early stopping. Depending on validation results, the learning rate gradually decreased after five epochs from its original value of 0.001 with a factor of 0.25. In order to build the proposed framework, Keras and TensorFlow are used as the backend. The NVIDIA K80 GPU is used to train all model variations.

B. Evaluation metrics

Every multi-class classification method is evaluated by the standard performance metrics [57]. Therefore, the following metrics are used in this study to assess the effectiveness of the methods: accuracy, F1 score, precision, sensitivity, specificity, and AUC (Area Under Curve). The value of performance measures is determined using the true positive (TP), false positive (FP), true negative (TN), and false negative (FN) predictions.

Accuracy: counts the number of accurate predictions made relative to all other predictions, it is frequently used as the basic measure for model evaluation [57]. It is calculated as

$$A_{cc} = \frac{TP + TN}{TP + TN + FP + FN}. \quad (7)$$

Precision: It is defined as the ratio of correctly classified positive samples (TP) to all positively classified samples (either correctly or incorrectly) [57]. Eq. 8 is used to calculate the precision of a method. Precision is important for medical image diagnosis as it highlights false positive cases.

$$P_r = \frac{TP}{TP + FP} \quad (8)$$

Sensitivity: The percentage of positive samples that were correctly classified as positive relative to all positive samples. The model’s sensitivity measures how effectively it can detect

positive samples [57]. Eq. 9 is used to calculate the sensitivity value. For medical image diagnosis, sensitivity is also an important measure. For better diagnosis, the value of false negatives in a CAD system should be minimum.

$$S_n = \frac{TP}{TP + FN} \quad (9)$$

F1 Score: Precision and recall are harmonically summed to produce the F1 score. It is a helpful measurement for datasets with imbalance distribution [57]. Eq. 10 is used to calculate the F1 score

$$F_1 = 2 * \frac{Precision \times Recall}{Precision + Recall}. \quad (10)$$

Specificity: The percentage of real negatives that the model successfully predicted [57]. Eq. 11 explains the specificity

$$S_p = \frac{TN}{TN + FP}. \quad (11)$$

Area Under Curve (AUC) refers to the evaluation result under the Receiver Operating Characteristic (ROC) curve. The AUC is the performance indicator for classification models at different threshold levels. The model’s ability to distinguish across classes are evaluated with the help of these measures.

C. Ablation study

We conducted an ablation study using the proposed methodology on the HAM10000 dataset to understand the impacts of each component of the proposed methodology, in particular the attention mechanism. We compare the baseline method, i.e., DenseNet-121 with two proposed class-wise attention variants. For the first variant, the proposed class-wise attention mechanism is employed after the baseline model’s fourth dense block. The second variant includes the class-wise attention mechanism at successive stages of the baseline model (i.e., after the 2nd, 3rd and 4th dense blocks), which we call progressive class-wise attention. The findings of the ablation study are displayed in Table II. To observe the confidence of the predictions of the progressive class-wise attention, we computed its five distinct runs on the HAM10000 dataset. The average results along with the standard deviation are presented

in Table III, which demonstrate the confidence of the proposed methodology on its predictions.

D. Results comparison with other attention mechanisms

Now we compare the performance of our approach with other state-of-the-art attention techniques. For a fair comparison, the attention mechanisms from the literature are employed at the same position in the DensNet architecture as the proposed class-wise attention. Table IV compares the outcomes of the attention technique for the HAM10000 dataset. The results demonstrate that the suggested attention performs effectively on the task of classifying skin lesions as compared with its counterparts. This improvement in performance is achieved while consuming fewer parameters as compared with the alternatives.

CBAM is a benchmark attention mechanism and has been employed in various methods targeted to diverse applications [58]–[60]. Table IV demonstrates how our proposed attention mechanism outperforms CBAM with fewer computational parameters in terms of accuracy, precision, recall, F1 score, and AUC. In comparison with CABNet our proposed method achieved competitive performance with a 1.1% improvement in precision with almost 2 million fewer parameters.

E. Comparison of the HAM10000 dataset’s results

The experimental findings of the suggested strategy for categorising exceedingly complex skin lesion types of the HAM10000 dataset are presented in this section. There are seven classes in this dataset that belong to dermoscopy images of resolution 450×600 . In Table V, the comparative analysis of the proposed method on the HAM10000 dataset is presented. We compared the proposed approach findings with existing approaches from literature and the top three positions on the ISIC archive leader board.

Meta-Optima’s [63] secured first place in the HAM10000 skin cancer categorization competition. Stacked ensemble CNN models are the foundation of the winner technique. The training set has been increased by the number of open-source skin cancer datasets, and several data augmentation techniques have been used. To address the issue of class imbalance, they have employed mini-batch, external data, and the inverse frequency, which selects the weight of the loss function. Our proposed method outperforms the ISIC leader-board winner with performance improvements of 1.7%, 18%, 16.9%, 18.3% and 1.5% in terms of accuracy, precision, sensitivity, F1 score and AUC, respectively.

Our proposed approach exceeded current state-of-the-art methods on the majority of performance metrics. The CAD [68] approach achieved the highest accuracy on the HAM10000 dataset. The CAD method used transfer learning, multi-layer feature fusion network and up-sampling and down-sampling approaches. The dual attention [25] method is used to channel spatial attention with auxiliary learning. To address the issue of imbalance the authors have also used an up-sampling approach. The FTN [66] and VIT Model [67] are transformer-based methods. The VIT model uses label shuffling and patch-based training to handle class imbalance.

The FTN method also used transfer learning for skin lesions classification. The MSM-CNN [9] employed three ensembles of learning-based CNN models to classify skin lesions. The authors employed external data and different sizes of cropped images for classification. FcResNet-TL [1] and Unit-wise [2] performed up-sampling and different data augmentations to enhance the data set.

To demonstrate the suggested model’s capacity for prediction and the interpretability of the attention processes, we utilized Grad-CAM [55]. The generated attention maps can assist dermatologists in analysing the lesion area for a particular class. In the first row of Figure 4, we present images from the HAM10000 data set that feature different classes. The second and third rows show the attention maps of the baseline and the proposed method, respectively. As seen in Figure 4, the model without attention mechanism emphasises on unwanted regions, hence missing important class-related feature information. Contrarily, the proposed framework concentrates on the important lesion areas that are necessary for robust skin cancer classification. Overall, the class activation maps demonstrate that the proposed approach extracts more precise lesion areas for diagnosis purposes.

F. Results comparison on the ISIC 2019 dataset

This section presents the experimental results of the proposed approach on ISIC 2019 dataset.

The findings of the proposed technique are compared with those of other state-of-the-art techniques in Table VI. The winner of the ISIC 2019 leaderboard used an ensemble approach and balancing loss to perform the classification of skin lesions. They also used different image resolutions, cropping and data augmentation approaches to enhance the data. Our proposed method surpassed in performance in comparison to the winner of the ISIC 2019 with improvements in terms of accuracy (0.1%), precision (55%), sensitivity (66%), F1 score (63.6%), specificity (1.8%) and AUC (5.6%).

The modified GoogleNet [56] achieved the results using transfer learning and by adding more filters in the architecture with up-sampling and down-sampling approaches. They achieved the best results by the down-sampling approach. Our proposed method achieves higher results in terms of precision (18%), sensitivity (18.8%), F1 score (18.2%) and specificity (2.4%). The author of Optimized DenseNet-201 [71] also used a balanced dataset for the evaluation of results with the modification in DenseNet architecture. The Fine-tuned DenseNet201 [70] method also uses up-sampling and down-sampling approaches with some image pre-processing techniques for classification tasks.

Table VI shows that the outcomes of the proposed technique on the ISIC2019 dataset are excellent. The proposed technique outperformed the comparison techniques in every performance measure.

In Figure 5, we present the attention maps of the ISIC 2019 dataset. In Figure 5, the first row represent the original images and the second row shows the attention maps of the proposed model. The proposed framework classification findings are well predictable since the activation maps concentrate clearly

Methods	A_{cc}	P_r	S_n	F_1	AUC	Parameters
DenseNet-121 (Baseline)	0.889	0.900	0.888	0.887	0.993	6.961 M
DenseNet-121+CBAM [61]	0.928	0.929	0.928	0.926	0.994	7.225 M
DenseNet-121+Soft Attention [62]	0.951	0.951	0.950	0.950	0.996	7.329 M
DenseNet-121+CABNet [49]	0.953	0.952	0.953	0.952	0.997	9.176 M
DenseNet-121+Class-wise Attention (ours)	0.958	0.963	0.957	0.957	0.997	7.085 M

TABLE IV: Proposed class-wise attention comparison with other attention mechanisms.

Methods	A_{cc}	P_r	S_n	F_1	AUC
Winner ISIC 2018 [63]	0.958	0.826	0.833	0.823	0.983
Runner-Up ISIC 2018 [64]	0.960	0.838	0.835	0.831	0.982
Rank3 ISIC 2018 [65]	0.954	0.794	0.830	0.805	0.980
Dual Attention [25]	0.896	-	0.817	-	0.983
FTN [66]	0.927	0.621	0.857	-	0.973
VIT Model [67]	0.941	0.942	-	0.941	0.987
MSM-CNN [9]	0.963	0.913	-	-	0.981
CAD [68]	0.981	0.935	0.934	0.934	0.965
FcResNet-TL [1]	0.961	0.960	0.964	0.961	0.984
Unit-wise [2]	0.981	0.911	0.972	0.973	0.984
Proposed (ours)	0.974	0.975	0.974	0.974	0.998

TABLE V: The results comparison on the HAM10000 data set.

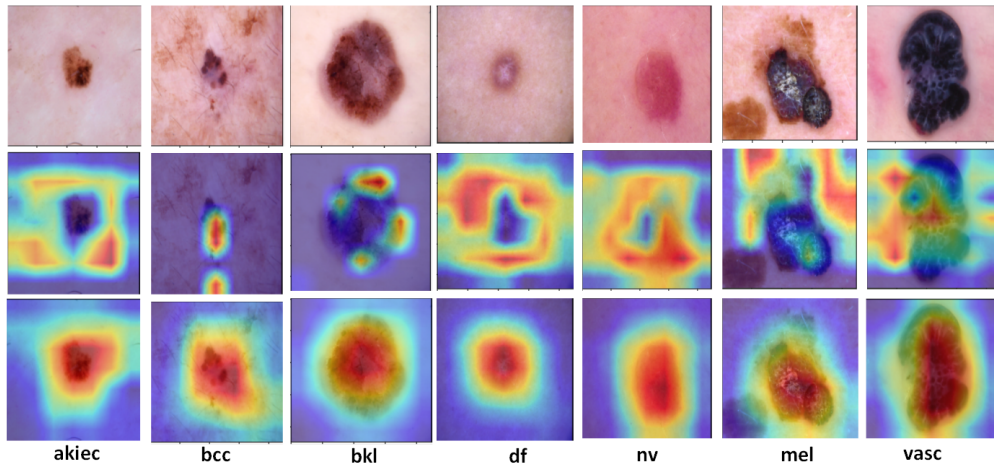


Fig. 4: Visualization results of each class on HAM10000 dataset. Original images are displayed in the first row, the second row shows the attention maps of the baseline model and the third row shows the attention maps of the proposed method.

on suspicious lesion regions, which will be helpful for clinical diagnosis.

The proposed strategy is thoroughly discussed in terms of numerical performances and visual outcomes. The proposed method achieved state-of-the-art results on both datasets owing to its class-wise attention mechanism that learns the features in a category-wise approach and treats every type of skin lesion in an identical manner. Since traditional CNN just stacks all the feature maps together without making any distinctions about classes, the information about the various categories is difficult to distinguish for correct classification. In order to lessen channel bias and expand the gap between distinct skin lesion classes, the proposed progressive class-wise attention assigns each type of skin lesion a certain number of feature channels and ensures that each skin lesion type has an equal number

of feature channels. From experimental results and attention maps, it can be seen that the proposed method produced state-of-the-art classification performance for skin lesions.

V. CONCLUSION

In this study, we present a progressive class-wise attention technique that is end-to-end trainable and has a strong generalisation of unseen data for the classification of skin lesions. The issue of high inter-class similarity, high intra-class variation, and class imbalance of skin lesions classification is addressed by the proposed technique. The proposed progressive class-wise attention focused on the discriminative areas of dermoscopic images to improve skin lesions classification performance. We employ Grad-CAM to gain insights into the proposed method's learned solutions and to aid clinical

Methods	A_{cc}	P_r	S_n	F_1	S_p	AUC
Winner ISIC 2019 [24]	0.940	0.609	0.571	0.578	0.975	0.941
Runner-Up ISIC 2019 [69]	0.932	0.515	0.661	0.567	0.951	0.807
Dual Attention [25]	0.890	-	0.835	-	0.979	0.976
Modified GoogleNet [56]	0.949	0.804	0.798	0.801	0.970	-
Fine-tuned DenseNet201 [70]	0.923	0.852	0.928	0.870	0.964	-
Optimized DenseNet-201 [71]	0.930	0.940	0.930	0.930	0.930	0.965
Proposed (ours)	0.949	0.949	0.948	0.947	0.993	0.994

TABLE VI: The results comparison on the ISIC 2019 data set.

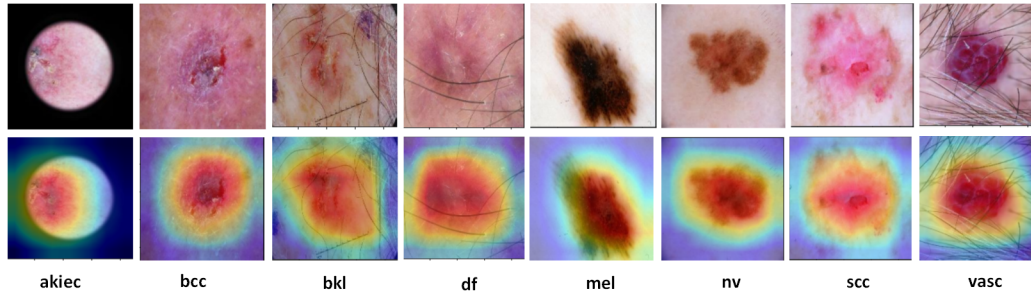


Fig. 5: Visualisation results of the ISIC 2019 dataset. The first row contains the original images, while the second row displays the outcomes of the proposed approach.

experts. Extensive analyses on two benchmark datasets for the classification of skin lesions are used to demonstrate the efficacy of the proposed approach. The efficiency of the proposed method can be enhanced through the incorporation of clinical data (e.g., age, sex, and body part information).

REFERENCES

- [1] I. Razzak, G. Shoukat, S. Naz, and T. M. Khan, "Skin lesion analysis toward accurate detection of melanoma using multistage fully connected residual network," in *2020 International Joint Conference on Neural Networks (IJCNN)*. IEEE, 2020, pp. 1–8.
- [2] I. Razzak and S. Naz, "Unit-wise: Deep shallow unit-wise residual neural networks with transition layer for expert level skin cancer classification," *IEEE/ACM Transactions on Computational Biology and Bioinformatics*, vol. 19, no. 02, pp. 1225–1234, mar 2022.
- [3] L. Siegel Rebecca, D. Miller Kimberly, E. Fuchs Hannah, and A. Jemal, "Cancer statistics, 2021," *CA Cancer J Clin*, vol. 71, no. 1, pp. 7–33, 2021.
- [4] J. Saeed and S. Zeebaree, "Skin lesion classification based on deep convolutional neural networks architectures," *Journal of Applied Science and Technology Trends*, vol. 2, no. 01, pp. 41–51, 2021.
- [5] E. Okur and M. Turkan, "A survey on automated melanoma detection," *Engineering Applications of Artificial Intelligence*, vol. 73, pp. 50–67, 2018.
- [6] M. Q. Khan, A. Hussain, S. U. Rehman, U. Khan, M. Maqsood, K. Mehmood, and M. A. Khan, "Classification of melanoma and nevus in digital images for diagnosis of skin cancer," *IEEE Access*, vol. 7, pp. 90 132–90 144, 2019.
- [7] M. Dildar, S. Akram, M. Irfan, H. U. Khan, M. Ramzan, A. R. Mahmood, S. A. Alsaiari, A. H. M. Saeed, M. O. Alraddadi, and M. H. Mahnashi, "Skin cancer detection: a review using deep learning techniques," *International journal of environmental research and public health*, vol. 18, no. 10, p. 5479, 2021.
- [8] M. Healsmith, J. Bourke, J. Osborne, and R. Graham-Brown, "An evaluation of the revised seven-point checklist for the early diagnosis of cutaneous malignant melanoma," *British Journal of Dermatology*, vol. 130, no. 1, pp. 48–50, 1994.
- [9] A. Mahbod, G. Schaefer, C. Wang, G. Dorffner, R. Ecker, and I. Ellinger, "Transfer learning using a multi-scale and multi-network ensemble for skin lesion classification," *Computer methods and programs in biomedicine*, vol. 193, p. 105475, 2020.
- [10] A. Khawaja, T. M. Khan, K. Naveed, S. S. Naqvi, N. U. Rehman, and S. J. Nawaz, "An improved retinal vessel segmentation framework using frangi filter coupled with the probabilistic patch based denoiser," *IEEE Access*, vol. 7, pp. 164 344–164 361, 2019.
- [11] A. Khawaja, T. M. Khan, M. A. Khan, and J. Nawaz, "A multi-scale directional line detector for retinal vessel segmentation," *Sensors*, vol. 19, no. 22, 2019.
- [12] T. M. Khan, A. Robles-Kelly, S. S. Naqvi, and A. Muhammad, "Residual multiscale full convolutional network (rm-fcn) for high resolution semantic segmentation of retinal vasculature," in *Structural, Syntactic, and Statistical Pattern Recognition: Joint IAPR International Workshops, S+SSPR 2020, Padua, Italy, January 21–22, 2021, Proceedings*. Springer Nature, 2021, p. 324.
- [13] T. M. Khan, M. A. Khan, N. U. Rehman, K. Naveed, I. U. Afridi, S. S. Naqvi, and I. Razzak, "Width-wise vessel bifurcation for improved retinal vessel segmentation," *Biomedical Signal Processing and Control*, vol. 71, p. 103169, 2022.
- [14] T. M. Khan, S. S. Naqvi, A. Robles-Kelly, and E. Meijering, "Neural network compression by joint sparsity promotion and redundancy reduction," in *Neural Information Processing: 29th International Conference, ICONIP 2022, Virtual Event, November 22–26, 2022, Proceedings, Part I*. Springer International Publishing Cham, 2023, pp. 612–623.
- [15] S. Iqbal, T. M. Khan, K. Naveed, S. S. Naqvi, and S. J. Nawaz, "Recent trends and advances in fundus image analysis: A review," *Computers in Biology and Medicine*, p. 106277, 2022.
- [16] T. M. Khan, M. Arsalan, I. Razzak, and E. Meijering, "Simple and robust depth-wise cascaded network for polyp segmentation," *Engineering Applications of Artificial Intelligence*, vol. 121, p. 106023, 2023.
- [17] S. S. Naqvi, Z. A. Langah, H. A. Khan, M. I. Khan, T. Bashir, M. Razzak, and T. M. Khan, "Glan: Gan assisted lightweight attention network for biomedical imaging based diagnostics," *Cognitive Computation*, vol. 15, no. 3, pp. 932–942, 2023.
- [18] T. M. Khan, S. S. Naqvi, A. Robles-Kelly, and I. Razzak, "Retinal vessel segmentation via a multi-resolution contextual network and adversarial learning," *Neural Networks*, 2023.
- [19] S. Iqbal, S. S. Naqvi, H. A. Khan, A. Saadat, and T. M. Khan, "G-net light: A lightweight modified google net for retinal vessel segmentation," in *Photonics*, vol. 9, no. 12. MDPI, 2022, p. 923.
- [20] S. Iqbal, K. Naveed, S. S. Naqvi, A. Naveed, and T. M. Khan, "Robust retinal blood vessel segmentation using a patch-based statistical adaptive multi-scale line detector," *Digital Signal Processing*, p. 104075, 2023.
- [21] R. B. Oliveira, J. P. Papa, A. S. Pereira, and J. M. R. Tavares, "Computational methods for pigmented skin lesion classification in images: review and future trends," *Neural Computing and Applications*, vol. 29, no. 3, pp. 613–636, 2018.

- [22] L. Bi, J. Kim, E. Ahn, and D. Feng, "Automatic skin lesion analysis using large-scale dermoscopy images and deep residual networks," *arXiv preprint arXiv:1703.04197*, 2017.
- [23] K. R. M. Fernando and C. P. Tsokos, "Dynamically weighted balanced loss: class imbalanced learning and confidence calibration of deep neural networks," *IEEE Transactions on Neural Networks and Learning Systems*, 2021.
- [24] N. Gessert, T. Sentker, F. Madesta, R. Schmitz, H. Kniep, I. Baltruschat, R. Werner, and A. Schlaefer, "Skin lesion classification using cnns with patch-based attention and diagnosis-guided loss weighting," *IEEE Transactions on Biomedical Engineering*, vol. 67, no. 2, pp. 495–503, 2019.
- [25] Z. Wei, Q. Li, and H. Song, "Dual attention based network for skin lesion classification with auxiliary learning," *Biomedical Signal Processing and Control*, vol. 74, p. 103549, 2022.
- [26] I. Gonzalez-Diaz, "Dermaknet: Incorporating the knowledge of dermatologists to convolutional neural networks for skin lesion diagnosis," *IEEE journal of biomedical and health informatics*, vol. 23, no. 2, pp. 547–559, 2018.
- [27] P. Tang, Q. Liang, X. Yan, S. Xiang, and D. Zhang, "Gp-cnn-dtel: Global-part cnn model with data-transformed ensemble learning for skin lesion classification," *IEEE Journal of Biomedical and Health Informatics*, vol. 24, no. 10, pp. 2870–2882, 2020.
- [28] K. M. Hosny, M. A. Kassem, and M. M. Foad, "Classification of skin lesions using transfer learning and augmentation with alex-net," *PLoS one*, vol. 14, no. 5, p. e0217293, 2019.
- [29] Y. Xie, J. Zhang, Y. Xia, and C. Shen, "A mutual bootstrapping model for automated skin lesion segmentation and classification," *IEEE Transactions on Medical Imaging*, vol. 39, no. 7, pp. 2482–2493, 2020.
- [30] Y. Liu, A. Jain, C. Eng, D. H. Way, K. Lee, P. Bui, K. Kanada, G. de Oliveira Marinho, J. Gallegos, S. Gabriele *et al.*, "A deep learning system for differential diagnosis of skin diseases," *Nature medicine*, vol. 26, no. 6, pp. 900–908, 2020.
- [31] A. Estava, B. Kuprel, R. Novoa, J. Ko, S. Swetter, H. Blau, and S. Thrun, "Dermatologist level classification of skin cancer with deep neural networks [j]," *Nature*, vol. 542, no. 7639, pp. 115–118, 2017.
- [32] T. M. Khan, S. S. Naqvi, and E. Meijering, "Leveraging image complexity in macro-level neural network design for medical image segmentation," *arXiv preprint arXiv:2112.11065*, 2021.
- [33] T. M. Khan, A. Robles-Kelly, and S. S. Naqvi, "T-Net: A Resource-Constrained Tiny Convolutional Neural Network for Medical Image Segmentation," in *Proceedings of the IEEE/CVF Winter Conference on Applications of Computer Vision*, 2022, pp. 644–653.
- [34] J. Deng, W. Dong, R. Socher, L.-J. Li, K. Li, and L. Fei-Fei, "Imagenet: A large-scale hierarchical image database," in *2009 IEEE conference on computer vision and pattern recognition*. Ieee, 2009, pp. 248–255.
- [35] L. Yu, H. Chen, Q. Dou, J. Qin, and P.-A. Heng, "Automated melanoma recognition in dermoscopy images via very deep residual networks," *IEEE transactions on medical imaging*, vol. 36, no. 4, pp. 994–1004, 2016.
- [36] J. Yang, X. Wu, J. Liang, X. Sun, M.-M. Cheng, P. L. Rosin, and L. Wang, "Self-paced balance learning for clinical skin disease recognition," *IEEE transactions on neural networks and learning systems*, vol. 31, no. 8, pp. 2832–2846, 2019.
- [37] A. Krizhevsky, I. Sutskever, and G. E. Hinton, "Imagenet classification with deep convolutional neural networks," *Advances in neural information processing systems*, vol. 25, 2012.
- [38] I. Radosavovic, R. P. Kosaraju, R. Girshick, K. He, and P. Dollár, "Designing network design spaces," in *Proceedings of the IEEE/CVF conference on computer vision and pattern recognition*, 2020, pp. 10 428–10 436.
- [39] M. Belkin, D. Hsu, S. Ma, and S. Mandal, "Reconciling modern machine-learning practice and the classical bias–variance trade-off," *Proceedings of the National Academy of Sciences*, vol. 116, no. 32, pp. 15 849–15 854, 2019.
- [40] S. S. Han, M. S. Kim, W. Lim, G. H. Park, I. Park, and S. E. Chang, "Classification of the clinical images for benign and malignant cutaneous tumors using a deep learning algorithm," *Journal of Investigative Dermatology*, vol. 138, no. 7, pp. 1529–1538, 2018.
- [41] D. Bisla, A. Choromanska, R. S. Berman, J. A. Stein, and D. Polsky, "Towards automated melanoma detection with deep learning: Data purification and augmentation," in *2019 IEEE/CVF Conference on Computer Vision and Pattern Recognition Workshops (CVPRW)*, 2019, pp. 2720–2728.
- [42] Y. Wang, M. Huang, X. Zhu, and L. Zhao, "Attention-based lstm for aspect-level sentiment classification," in *Proceedings of the 2016 conference on empirical methods in natural language processing*, 2016, pp. 606–615.
- [43] H. Chen, M. Sun, C. Tu, Y. Lin, and Z. Liu, "Neural sentiment classification with user and product attention," in *Proceedings of the 2016 conference on empirical methods in natural language processing*, 2016, pp. 1650–1659.
- [44] H. Xia, Y. Luo, and Y. Liu, "Attention neural collaboration filtering based on gru for recommender systems," *Complex & Intelligent Systems*, vol. 7, no. 3, pp. 1367–1379, 2021.
- [45] F. Wang, M. Jiang, C. Qian, S. Yang, C. Li, H. Zhang, X. Wang, and X. Tang, "Residual attention network for image classification," in *Proceedings of the IEEE conference on computer vision and pattern recognition*, 2017, pp. 3156–3164.
- [46] J. Hu, L. Shen, and G. Sun, "Squeeze-and-excitation networks," in *Proceedings of the IEEE conference on computer vision and pattern recognition*, 2018, pp. 7132–7141.
- [47] J. Zhang, Y. Xie, Y. Xia, and C. Shen, "Attention residual learning for skin lesion classification," *IEEE transactions on medical imaging*, vol. 38, no. 9, pp. 2092–2103, 2019.
- [48] X. He, Y. Wang, S. Zhao, and C. Yao, "Deep metric attention learning for skin lesion classification in dermoscopy images," *Complex & Intelligent Systems*, vol. 8, no. 2, pp. 1487–1504, 2022.
- [49] A. He, T. Li, N. Li, K. Wang, and H. Fu, "Cabnet: category attention block for imbalanced diabetic retinopathy grading," *IEEE Transactions on Medical Imaging*, vol. 40, no. 1, pp. 143–153, 2020.
- [50] P. Tschandl, C. Rosendahl, and H. Kittler, "The ham10000 dataset, a large collection of multi-source dermatoscopic images of common pigmented skin lesions," *Scientific data*, vol. 5, no. 1, pp. 1–9, 2018.
- [51] M. Combalia, N. C. Codella, V. Rotemberg, B. Helba, V. Vilaplana, O. Reiter, C. Carrera, A. Barreiro, A. C. Halpern, S. Puig *et al.*, "Bcn20000: Dermoscopic lesions in the wild," *arXiv preprint arXiv:1908.02288*, 2019.
- [52] N. C. Codella, D. Gutman, M. E. Celebi, B. Helba, M. A. Marchetti, S. W. Dusza, A. Kalloo, K. Liopyris, N. Mishra, H. Kittler *et al.*, "Skin lesion analysis toward melanoma detection: A challenge at the 2017 international symposium on biomedical imaging (isbi), hosted by the international skin imaging collaboration (isic)," in *2018 IEEE 15th international symposium on biomedical imaging (ISBI 2018)*. IEEE, 2018, pp. 168–172.
- [53] G. Huang, Z. Liu, L. Van Der Maaten, and K. Q. Weinberger, "Densely connected convolutional networks," in *Proceedings of the IEEE conference on computer vision and pattern recognition*, 2017, pp. 4700–4708.
- [54] T.-Y. Lin, P. Goyal, R. Girshick, K. He, and P. Dollár, "Focal loss for dense object detection," *IEEE Transactions on Pattern Analysis and Machine Intelligence*, vol. 42, no. 2, pp. 318–327, 2020.
- [55] R. R. Selvaraju, M. Cogswell, A. Das, R. Vedantam, D. Parikh, and D. Batra, "Grad-cam: Visual explanations from deep networks via gradient-based localization," in *Proceedings of the IEEE international conference on computer vision*, 2017, pp. 618–626.
- [56] M. A. Kassem, K. M. Hosny, and M. M. Foad, "Skin lesions classification into eight classes for isic 2019 using deep convolutional neural network and transfer learning," *IEEE Access*, vol. 8, pp. 114 822–114 832, 2020.
- [57] M. Grandini, E. Bagli, and G. Visani, "Metrics for multi-class classification: an overview," *arXiv preprint arXiv:2008.05756*, 2020.
- [58] P. Alirezazadeh, M. Schirrmann, and F. Stolzenburg, "Improving deep learning-based plant disease classification with attention mechanism," *Gesunde Pflanzen*, pp. 1–11, 2022.
- [59] S. Yu, S. Jin, J. Peng, H. Liu, and Y. He, "Application of a new deep learning method with cbam in clothing image classification," in *2021 IEEE International Conference on Emergency Science and Information Technology (ICESIT)*. IEEE, 2021, pp. 364–368.
- [60] X. Li, H. Xia, and L. Lu, "Eca-cbam: Classification of diabetic retinopathy: Classification of diabetic retinopathy by cross-combined attention mechanism," in *2022 the 6th International Conference on Innovation in Artificial Intelligence (ICIAI)*, 2022, pp. 78–82.
- [61] S. Woo, J. Park, J.-Y. Lee, and I. S. Kweon, "Cbam: Convolutional block attention module," in *Proceedings of the European conference on computer vision (ECCV)*, 2018, pp. 3–19.
- [62] S. K. Datta, M. A. Shaikh, S. N. Srihari, and M. Gao, "Soft attention improves skin cancer classification performance," in *Interpretability of Machine Intelligence in Medical Image Computing, and Topological Data Analysis and Its Applications for Medical Data*. Springer, 2021, pp. 13–23.
- [63] A. Nozdryn-Plotnicki, J. Yap, and W. Yolland, "Ensembling convolutional neural networks for skin cancer classification," *International Skin*

Imaging Collaboration (ISIC) Challenge on Skin Image Analysis for Melanoma Detection. MICCAI, 2018.

- [64] N. Gessert, T. Sentker, F. Madesta, R. Schmitz, H. Kniep, I. Baltruschat, R. Werner, and A. Schlaefer, "Skin lesion diagnosis using ensembles, unscaled multi-crop evaluation and loss weighting," *arXiv preprint arXiv:1808.01694*, 2018.
- [65] J. Zhuang, W. Li, S. Manivannan, R. Wang, J. Zhang, J. Pan, G. Jiang, and Z. Yin, "Skin lesion analysis towards melanoma detection using deep neural network ensemble," *ISIC Challenge*, vol. 2018, no. 2, pp. 1–6, 2018.
- [66] X. He, E.-L. Tan, H. Bi, X. Zhang, S. Zhao, and B. Lei, "Fully transformer network for skin lesion analysis," *Medical Image Analysis*, vol. 77, p. 102357, 2022.
- [67] C. Xin, Z. Liu, K. Zhao, L. Miao, Y. Ma, X. Zhu, Q. Zhou, S. Wang, L. Li, F. Yang *et al.*, "An improved transformer network for skin cancer classification," *Computers in Biology and Medicine*, p. 105939, 2022.
- [68] I. Bakkouri and K. Afdel, "Computer-aided diagnosis (cad) system based on multi-layer feature fusion network for skin lesion recognition in dermoscopy images," *Multimedia Tools and Applications*, vol. 79, no. 29, pp. 20 483–20 518, 2020.
- [69] S. Zhou, Y. Zhuang, and R. Meng, "Multi-category skin lesion diagnosis using dermoscopy images and deep cnn ensembles," *DysionAI, Tech. Rep.*, 2019.
- [70] S. Benyahia, B. Meftah, and O. L  zoray, "Multi-features extraction based on deep learning for skin lesion classification," *Tissue and Cell*, vol. 74, p. 101701, 2022.
- [71] J. P. Villa-Pulgarin, A. A. Ruales-Torres, D. Arias-Garzon, M. A. Bravo-Ortiz, H. B. Arteaga-Arteaga, A. Mora-Rubio, J. A. Alzate-Grisales, E. Mercado-Ruiz, M. Hassaballah, S. Orozco-Arias *et al.*, "Optimized convolutional neural network models for skin lesion classification," *Comput. Mater. Contin.*, vol. 70, no. 2, pp. 2131–2148, 2022.